THE JOURNAL OF BIOLOGICAL CHEMISTRY VOL. 285, NO. 23, pp. 17907–17917, June 4, 2010

The Metabotropic Glutamate Receptor mGlu7 Activates Phospholipase C, Translocates Munc-13-1 Protein, and Potentiates Glutamate Release at Cerebrocortical Nerve Terminals*

Received for publication, October 30, 2009, and in revised form, March 11, 2010 Published, JBC Papers in Press, April 7, 2010, DOI 10.1074/jbc.M109.080838

Ricardo Martín[‡], Thierry Durroux[§], Francisco Ciruela[¶], Magdalena Torres[‡], Jean-Philippe Pin[§], and José Sánchez-Prieto[‡1]

From the [‡]Departamento de Bioquímica, Facultad de Veterinaria, Universidad Complutense, 28040 Madrid, Spain, the [§]Centre National de la Recherche Scientifique (CNRS), UMR 5203, Institut de Génomique Fonctionnelle, 141 Rue de la Cardonille, Montpellier F-34000, France, and the [¶]Unitat de Farmacologia, Departament Patologia i Terapèutica Experimental, Facultat de Medicina, Universitat de Barcelona, L'Hospitalet de Llobregat, 08907 Barcelona, Spain

At synaptic boutons, metabotropic glutamate receptor 7 (mGlu7 receptor) serves as an autoreceptor, inhibiting glutamate release. In this response, mGlu7 receptor triggers pertussis toxin-sensitive G protein activation, reducing presynaptic Ca^{2+} influx and the subsequent depolarization evoked release. Here we report that receptor coupling to signaling pathways that potentiate release can be seen following prolonged exposure of nerve terminals to the agonist L-(+)-phosphonobutyrate, L-AP4. This novel mGlu7 receptor response involves an increase in the release induced by the Ca^{2+} ionophore ionomycin, suggesting a mechanism that is independent of Ca^{2+} channel activity, but dependent on the downstream exocytotic release machinery. The mGlu7 receptor-mediated potentiation resists exposure to pertussis toxin, but is dependent on phospholipase C, and increased phosphatidylinositol (4,5)-bisphosphate hydrolysis. Furthermore, the potentiation of release does not depend on protein kinase C, although it is blocked by the diacylglycerol-binding site antagonist calphostin C. We also found that activation of mGlu7 receptors translocate the active zone protein essential for synaptic vesicle priming, munc13-1, from soluble to particulate fractions. We propose that the mGlu7 receptor can facilitate or inhibit glutamate release through multiple pathways, thereby exerting homeostatic control of presynaptic function.

Metabotropic glutamate receptors belong to the G protein-coupled receptors (GPCRs)[2] superfamily and their eight receptor subtypes (mGlu1–8 receptors) are classified into three major groups. Most group III mGlu receptors (mGlu4, -6, -7, and -8 receptors) are located within the presynaptic active zone (1) where they act as autoreceptors mediating feedback inhibition of glutamate release (2–4). The signaling mechanism initiated by mGlu7 receptors to inhibit neurotransmitter release involves the activation of $G_{i/o}$ proteins that inhibit Ca^{2+} channels and adenylyl cyclase (5), and probably the release process itself (6). However, mGlu7 receptor signaling is not restricted to these pathways. Thus, transfected mGlu7 receptors expressed in cerebellar granule cells inhibits somatic Ca^{2+} currents by a mechanism that involves the activation of phospholipase C (PLC) and the hydrolysis of phosphatidylinositol (4,5)-bisphosphate thereby generating inositol trisphosphate that releases Ca^{2+} from intracellular stores and diacylglycerol (DAG) that activates protein kinase C (PKC) (7). However, one important question that remains to be resolved is whether endogenous mGlu7 receptors at synaptic sites also signal via PLC and if so, what effect such signaling has on release modulation.

Phorbol esters, stable analogues of the endogenous product of PLC, DAG, potentiate synaptic transmission by increasing neurotransmitter release (8–15). DAG signaling at synapses has long been thought to be mediated by PKC and both presynaptic K^+ and Ca^{2+} channels, as well as other proteins of the release machinery, have been identified as PKC substrates. In addition to PKC activation, phorbol esters can also activate munc13-1, a presynaptic protein with an essential role in synaptic vesicle priming (16, 17). However, there is little information regarding the presynaptic receptors coupled to signaling pathways involved in synaptic potentiation. Presynaptic PLC activation in response to high frequency stimulation results in synaptic potentiation due to increased neurotransmitter release in hippocampal neurons (18). As high frequency stimulation increases synaptic glutamate enough to activate low affinity mGlu7 receptors (19), it remains unclear whether

* This work was supported by Spanish Ministerio de Educación y Ciencia Grant BFU2007-64154/BFI, Instituto de Salud Carlos III Grant RD06/0026, and Comunidad de Madrid Grants S-BIO-0170/2006 (to J. S.-P.) and SAF2008-01462, and Consolider-Ingenio CSD2008-00005 from the Ministerio de Ciencia e Innovación (to F. C.).

[1] To whom correspondence should be addressed. Tel.: 34-1-394-3891; Fax: 34-91-394-3909; E-mail: jsprieto@vet.ucm.

[2] The abbreviations used are: GPCR, G protein-coupled receptor; mGlu7 receptor, metabotropic glutamate receptor 7; L-AP4, L-(+)-phosphonobutyrate; PLC, phospholipase C; PKC, protein kinase C; DAG, diacylglycerol; PTX, pertussis toxin; HBM, HEPES-buffered medium; BSA, bovine serum albumin; fura2-AM, fura2-acetoxymethyl ester; IP_1, inositol monophosphate; TBS, Tris-buffered saline; vGluT1, vesicular glutamate transporter 1; AChase, acetylcholinesterase; LDH, lactic dehydrogenase; CPPG, (*R*,*S*)-α-cyclipropyl-4-phosphono-phenylglycine; PKA, cAMP-dependent protein kinase; CPCCOEt, 7-(hydroxyimino)cyclopropa[*b*]chromen-1a-carboxylate ethyl ester; GIRK, G protein-coupled inward rectifier K channels; HFS, high frequency stimulation; RIM1α, Rab3A-interacting protein; $[Ca^{2+}]_c$, cytosolic free Ca^{2+} concentration.

mGlu7 receptors may activate presynaptic PLC and whether this action enhances glutamate release.

Here we show, in a preparation of cerebrocortical nerve terminals, that mGlu7 receptors inhibit the release process, but can also potentiate it under specific conditions. Indeed, release potentiation is observed after a prolonged exposure of the receptor to agonist L-AP4. The new signaling elicited by the receptor involves PLC activation via a pertussis toxin (PTX)-insensitive G protein and the subsequent hydrolysis of phosphatidylinositol (4,5)-bisphosphate. The mGlu7 receptor-dependent response potentiates release by a mechanism that could be dependent on the downstream release machinery because a parallel translocation of the active zone munc13-1 protein from the soluble to particulate fractions is observed upon receptor activation.

EXPERIMENTAL PROCEDURES

Synaptosomal Preparation—The handling and all procedures to sacrifice the animals used in this study were performed in accordance to the European Commission guidelines (86/609/CEE) and approved by the Animal Research Committee at the Complutense University. Synaptosomes were purified on discontinuous Percoll gradients (Amersham Biosciences) as described previously (5). Briefly, the cerebral cortex was isolated from adult male Wistar rats (2–3 months old) and homogenized in medium containing 0.32 M sucrose (pH 7.4). The homogenate was centrifuged for 2 min at 2,000 × *g* and 4 °C, and the supernatant spun again at 9,500 × *g* for 12 min. From the pellets formed, the white loosely compacted layer containing the majority of the synaptosomes was gently resuspended in 8 ml of 0.32 M sucrose (pH 7.4). An aliquot of this synaptosomal suspension (2 ml) was placed onto a 3-ml Percoll discontinuous gradient containing: 0.32 M sucrose, 1 mM EDTA, 0.25 mM DL-dithiothreitol, and 3, 10, or 23% Percoll (pH 7.4). After centrifugation at 25,000 × *g* for 10 min at 4 °C, the synaptosomes were recovered from the 10 and 23% Percoll bands, and they were diluted in a final volume of 30 ml of HEPES buffer medium (HBM): 140 mM NaCl, 5 mM KCl, 5 mM $NaHCO_3$, 1.2 mM NaH_2PO_4, 1 mM $MgCl_2$, 10 mM glucose, and 10 mM HEPES (pH 7.4). Following further centrifugation at 22,000 × *g* for 10 min, the synaptosome pellet was resuspended in 6 ml of HBM and the protein content was determined by the Biuret method. Finally, 1 mg of the synaptosomal suspension was diluted in 2 ml of HBM and spun at 3,000 × *g* for 10 min. The supernatant was discarded and the pellets containing the synaptosomes were stored on ice. Under these conditions the synaptosomes remain fully viable for at least 4–6 h, as judged by the extent of KCl-evoked glutamate release.

Glutamate Release—Glutamate release was assayed by online fluorimetry as described previously (5). Synaptosomal pellets were resuspended in HBM (0.67 mg/ml) and preincubated at 37 °C for 1 h in the presence of 16 μM bovine serum albumin (BSA) to bind any free fatty acids released from synaptosomes during the preincubation (20). A 1-ml aliquot was transferred to a stirred cuvette containing 1 mM $NADP^+$, 50 units of glutamate dehydrogenase (Sigma), and 1.33 mM $CaCl_2$ or 200 nM free Ca^{2+}, and the fluorescence of NADPH was followed in a PerkinElmer LS-50 luminescence spectrometer at excitation and emission wavelengths of 340 and 460 nm, respectively. Traces were calibrated by the addition of 2 nmol of glutamate at the end of each assay. The data were obtained at 2-s intervals and corrected for Ca^{2+}-independent release. Accordingly, the Ca^{2+}-dependent release was calculated by subtracting the release obtained during a 5-min period of depolarization at 200 nM free [Ca^{2+}] from the release at 1.33 mM $CaCl_2$.

The Cytosolic Free Ca^{2+} Concentration ([Ca^{2+}]$_c$) in the Synaptosomal Population—The $[Ca^{2+}]_c$ concentration was measured with fura2. Synaptosomes were resuspended in HBM (2 mg/ml) with 16 μM BSA in the presence of 1.3 mM $CaCl_2$ and 5 μM fura2-acetoxymethyl ester (fura2-AM; Molecular Probes, Eugene, OR), and incubated at 37 °C for 25 min. After fura2 loading, the synaptosomes were pelleted and resuspended in fresh HBM with BSA. A 1-ml aliquot was transferred to a stirred cuvette containing 1.3 mM $CaCl_2$ and the fluorescence was monitored at 340 and 510 nm. Data points were taken at 0.5-s intervals and the $[Ca^{2+}]_{cyt}$, was calculated using the equations described previously (21).

IP_1 Accumulation—IP_1 accumulation was determined using the IP-One kit (Cisbio, Bioassays, Bagnol sur-Cèze, France) (22). Synaptosomes (0.67 mg/ml) in HBM with 16 μM BSA and adenosine deaminase (1.25 units/mg of protein) were incubated for 1 h at 37 °C. After 25 min 50 mM LiCl was added to inhibit inositol monophosphatase and subsequently the agonist L-AP4 was added for 20 min prior to lysis. Other drugs were added as indicated in the figure legends. Synaptosomes were collected by centrifugation at 13,000 × *g* for 1 min at 4 °C and resuspended (1 mg/0.1 ml) in lysis buffer: 50 mM HEPES, 0.8 M potassium fluoride, 0.2% (w/v) BSA, and 1% (v/v) Triton X-100, pH 7.0). The lysed synaptosomes were transferred to a 96-well assay plate and the homogeneous time-resolved fluorescence (HTRF) components were added: the europium cryptate-labeled anti-IP_1 antibody, and the d2-labeled IP_1 analogue were both diluted in lysis buffer. After incubating the assays for 1 h at room temperature, the europium cryptate fluorescence and the time-resolved fluorescence resonance energy transfer signals were measured 50 μs after excitation at 337 at both 620 and 665 nm, respectively, using a RubyStar fluorimeter (BMG Labtechnologies, Offenburg, Germany). The fluorescence intensities measured at 620 and 665 nm correspond to the total europium cryptate emission and the FRET signal, respectively. The specific FRET signal was calculated using the following equation: $\Delta F\% = 100 \times (R_{pos} - R_{neg})/(R_{neg})$, where R_{pos} is the fluorescence ratio (665/620 nm) calculated in the wells incubated with both donor- and acceptor-labeled antibodies, and R_{neg} is the same ratio for the negative control incubated only with the donor fluorophore-labeled antibody. The FRET signal ($\Delta F\%$), which is inversely proportional to the concentration of IP_1 in the cells, was then transformed into the accumulated IP_1 value using a calibration curve prepared on the same plate.

cAMP Accumulation— cAMP accumulation was determined using a cAMP dynamic kit (Cisbio, Bioassays, Bagnol sur-Cèze, France). The assay was similar to that described for IP_1 except that during incubation the cAMP phosphodiesterase inhibitor Ro-20-1724 (0.1 mM) (Calbiochem, Damstard, Germany) was included for 35 min during incubation. The homogeneous time-resolved fluorescence assay was also similar to that

described for IP_1 except that an anti-cAMP antibody and d2-labeled cAMP analogue were used.

Immunocytochemistry—The affinity purified guinea pig polyclonal antisera against mGlu4a, mGlu7a, and mGlu8a receptors used here have been described elsewhere (23). The polyclonal rabbit antiserum against synaptophysin 1 was obtained from Synaptic Systems, Gottingen, Germany. As a control of the immunochemical reactions, primary antibodies were omitted from the staining procedure whereupon no immunoreactivity could be detected that resembled that obtained with the specific antibodies.

Immunocytochemical Procedures—The synaptosomes were allowed to attach to polylysine-coated coverslips for 1 h and then fixed for 5 min in 4% paraformaldehyde in 0.1 M phosphate buffer (pH 7.4). Following several washes with 0.1 M phosphate buffer (pH 7.4), the synaptosomes were preincubated for 1 h in 10% normal goat serum diluted in 50 mM Tris buffer (pH 7.4) containing 0.9% NaCl (TBS) and 0.2% Triton X-100. Subsequently, they were then incubated for 24 h with the appropriate primary antiserum diluted in TBS with 1% normal goat serum and 0.2% Triton X-100:mGlu7a (1 μg/ml), mGlu4a (1 μg/ml), mGlu8a (1 μg/ml) receptors, or synaptophysin (1:100). After washing in TBS, the synaptosomes were incubated with secondary antibodies diluted in TBS for 2 h: a goat anti-rabbit antibody coupled to the Cy2 cyanine-derived fluorochrome Cy2 (diluted 1:200; Jackson, West Grove, PA) or a Cy3-coupled donkey anti-guinea pig antibody (diluted 1:400, Chemicon International, Temecula, CA). After several washes in TBS, the coverslips were mounted with Prolong Antifade Kit (Molecular Probes) and the synaptosomes were viewed with a Nikon Diaphot microscope equipped with a ×100 objective, a mercury lamp light source, and fluorescein-rodamine Nikon filter sets.

Munc13-1 Translocation—Synaptosomes were resuspended (0.67 mg/ml) in HMB medium with 16 μM BSA and incubated for 30 min at 37 °C. Adenosine deaminase (1.25 units/mg of protein) was then added for another 20 min, followed by L-AP4 1 mM for 10 min. Synaptosomes were washed by centrifugation (13,000 × *g* for 1 min) and resuspended (2 mg/ml) in hypoosmotic medium (Tris-HCl buffer, 8.3 mM, pH 7.4) containing Protease Inhibitor Mixture Kit (Thermo Scientific, Rockford, IL). The synaptosomal suspension was passed through a 20-gauge syringe to disaggregate the synaptosomes and maintained at 4 °C for 30 min with gentle shaking. After this time the soluble and particulate fractions were separated by centrifugation at 40,000 × *g* for 10 min. The supernatant (soluble fraction) was collected and the pellet (particulate fraction) was resuspended in RIPA buffer (1% Triton X-100, 0.5% deoxycholate, 0.2% SDS, 100 mM NaCl, 1 mM EDTA, 50 mM Tris-HCl, pH 7.4). Soluble and particulate fractions were used to assess enzymatic activity (acetylcholinesterase and lactic dehydrogenase, LDH) or for SDS-PAGE electrophoresis and Western blotting (Munc13-1; vGluT1 and Na,K-ATPase, β subunit). Acetylcholinesterase activity was determined fluorometrically by the Ellman's reaction in the presence of 0.75 mM acetylthiocholine iodide, 0.2 mM 5,5′-dithiobis(2-nitrobenzoic acid), and 100 mM potassium phosphate buffer (pH 8). LDH activity was assayed following NADH oxidation in medium containing 1 mM pyruvate, 0.2 mM NADH, 50 mM potassium phosphate buffer (pH 7.4) in the presence of 0.5% (v/v) Triton X-100. Soluble and particulate fractions (3 μg of protein per lane) were diluted in Laemmli loading buffer with β-mercaptoethanol (5% v/v), resolved in SDS-PAGE (7.5% acrylamide, Bio-Rad), and analyzed by Western blotting according to standard procedures. All samples were normalized to the levels of β-tubuline (soluble and particulate fractions) in the same blot as a loading control. Goat anti-rabbit and goat anti-mouse secondary antibodies coupled to Odyssey IRDye 680 or Odyssey IRDye 800 (Rockland Immunochemicals, Gilbertsville, PA) were used for quantitative Western blotting using the Odyssey System (LI-COR, Lincoln, NE). The following primary antibodies were used to probe Western blots: polyclonal rabbit anti-Munc13-1 (1:1000), monoclonal mouse anti-Munc13-1 (1:200), polyclonal rabbit anti-vGluT1 serum (1:7000 Synaptic Systems, Germany), monoclonal mouse anti-β-tubulin (1.2000 Sigma), and polyclonal rabbit anti-Na,K-ATPase-β_1-subunit (1:3500 Millipore, Molshein, France).

Co-immunoprecipitation—The primary antibodies used for immunoprecipitations were a mouse monoclonal anti-munc13-1 (Synaptic Systems, Gottingem, Germany) or an affinity purified rabbit polyclonal antiserum against mGlu7a receptor (23). The secondary antibodies were horseradish peroxidase-conjugated anti-rabbit IgG TrueBlot™ (1:1000; eBioscience, San Diego, CA). The proteins recovered were resolved by SDS-PAGE on 6.5% polyacrylamide gels and transferred to polyvinylidene difluoride membranes using a semi-dry transfer system, which were then probed with the antibody indicated and a horseradish peroxidase-conjugated secondary antibody. The immunoreactive bands were visualized by chemiluminescence (Pierce) and detected in a LAS-3000 (FujiFilm Life Science, Woodbridge, CT). P_2 synaptosomes isolated from adult rats (Wistar) were homogenized using a VDI 12 homogenizer (VWR International, Barcelona, Spain) and solubilized for 30 min on ice in radioimmunoprecipitation assay (RIPA) buffer (50 mM Tris-HCl, pH 7.4, 100 mM NaCl, 1% Triton X-100, 0.5% sodium deoxycholate, 0.2% SDS, and 1 mM EDTA) for 30 min on ice. The solubilized preparation was then centrifuged at 13,000 × *g* for 30 min and the supernatant (2 mg/ml) was processed for immunoprecipitation, each step was conducted with constant rotation at 0–4 °C. The supernatant was incubated overnight with the antibody indicated and then 50 μl of a suspension of either protein A cross-linked to agarose beads (Sigma) or TrueBlot anti-rabbit Ig IP beads (eBioscience, San Diego, CA) was added and the mixture and incubated overnight. Subsequently, the beads were washed with ice-cold RIPA buffer that was removed with a 28-gauge needle. Then, 100 μl of SDS-PAGE sample buffer (0.125 M Tris-HCl, pH 6.8, 4% SDS, 20% glycerol, 0.004% bromphenol blue) was added to each sample, and the immune complexes were dissociated by adding fresh dithiothreitol (50 mM final concentration) and heating to 90 °C for 10 min. Proteins were resolved and detected as described above.

RESULTS

Release Inhibition—It is known that mGlu7 receptors inhibit synaptic transmission by decreasing evoked glutamate release and Ca^{2+} influx (5). The cerebrocortical nerve terminal prepa-

ration from adult rats is enriched in this receptor, as witnessed by co-labeling with antisera against the vesicle marker synaptophysin and the L-AP4-sensitive mGlu receptors (4, 7, and 8) expressed in the brain. Indeed, among the nerve terminals that contained synaptophysin (1,148 particles from 7 fields), 30.0 ± 1.2% also contained mGlu7a receptor (mean ± S.E.; Fig. 1, *A* and *D*), whereas only 1.4 ± 0.5% contained mGluR4a (1,616 particles from 8 fields) and 1.6 ± 0.6% (989 particles from 8 fields) were immunoreactive for mGlu4a and mGlu8a receptors, respectively (Fig. 1, *B–D*). Thus the responses to L-AP4 are largely mediated by the mGlu7 receptor in this preparation.

Depolarization of nerve terminals with KCl increases Ca^{2+} influx and glutamate release (5). In naive synaptosomes, the glutamate release evoked by 30 mM KCl (2.7 ± 0.1 nmol of Glu/mg of protein ± S.E., $n = 6$) fell to 66.7 ± 5% of control value in the presence of the group III mGlu receptor agonist, L-AP4 ($n = 6$, $p < 0.001$, Fig. 1, *E* and *F*). This response paralleled the reduction in depolarization-induced Ca^{2+} influx to 81.8 ± 1.2% of that in the controls ($n = 8$, $p < 0.01$, Fig. 1, *G* and *H*). However, there was no reduction in KCl-evoked release (97.0 ± 2% of control release) in synaptosomes that were exposed to L-AP4 (1 mM) for 10 min ($n = 8$, $p > 0.05$, Fig. 1, *E* and *F*). It is possible that the mGlu7 receptor undergoes activity-dependent internalization (19, 24, 25), leading to loss of the receptor response. However, this second agonist addition still decreased the Ca^{2+}-influx in fura2-loaded synaptosomes (81.40 ± 1%, $n = 8$, $p < 0.01$, Fig. 1, *G* and *H*), indicating that the mGlu7 receptor remains at the surface and therefore that such receptor failure to reduce the evoked release is not due to receptor internalization. It is also possible that prolonged exposure to L-AP4 promotes a new response that augments release thereby counterbalancing the inhibition due to diminished Ca^{2+} influx. Because 30 mM

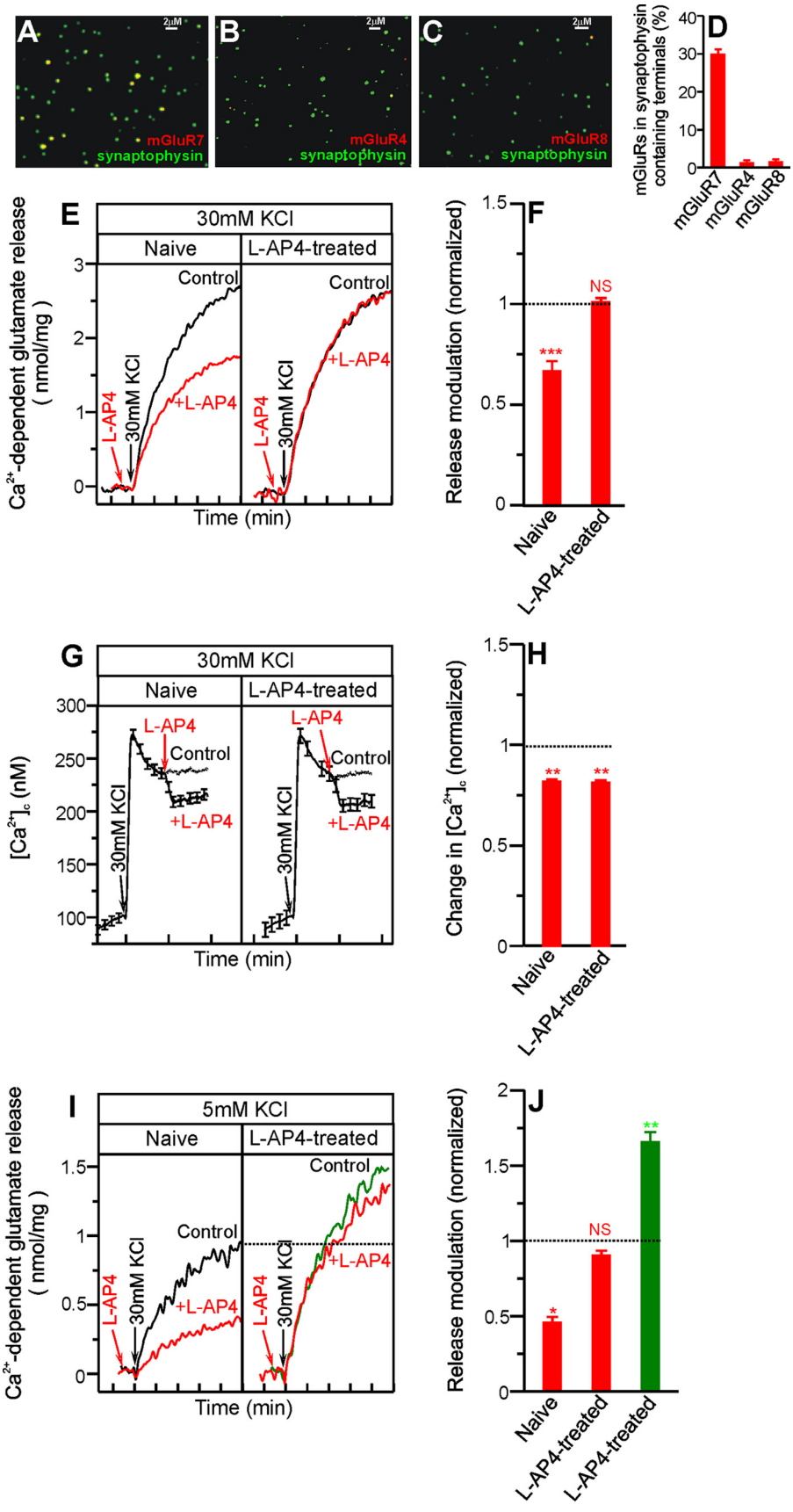

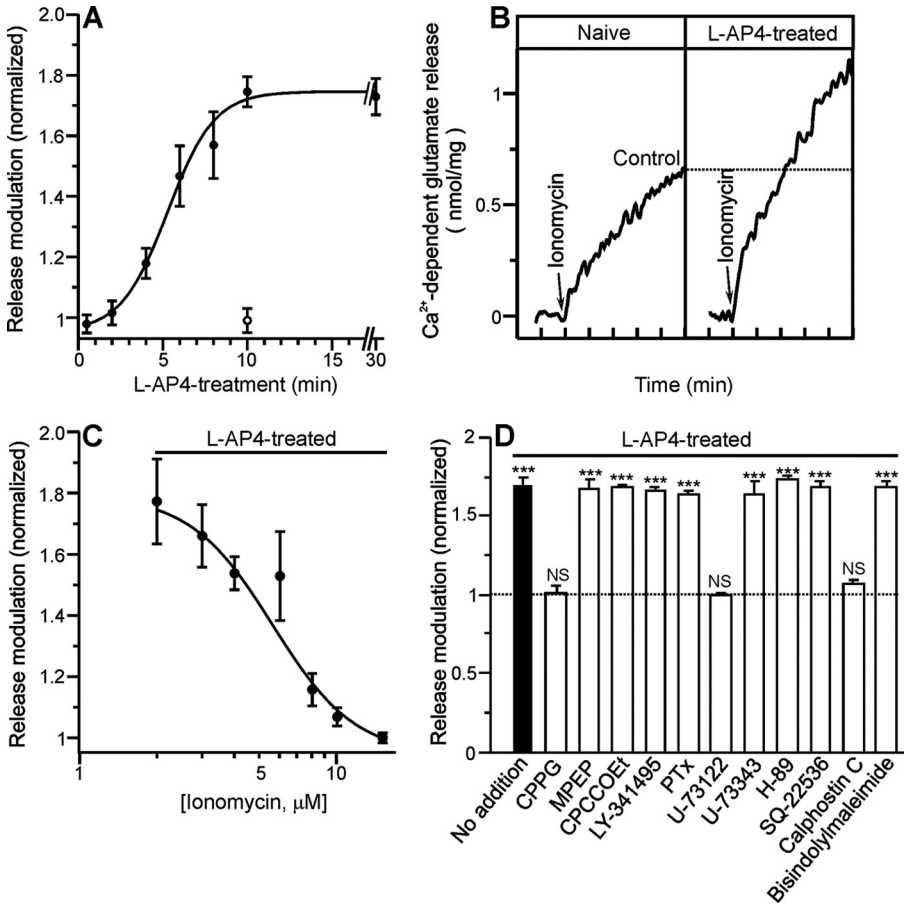

FIGURE 2. **Pharmacology of the L-AP4-induced release potentiation.** *A*, time course of the L-AP4 treatment in release facilitation. Nerve terminals were exposed to L-AP4 (1 mM) for the indicated times (*closed symbols*) and then washed, centrifuged, and resuspended to remove the agonist. Ionomycin-induced release was determined and compared with that obtained in non-treated synaptosomes. *Open symbol* indicates the release facilitation after treatment with L-AP4 (20 μM, 10 min). *B*, glutamate release induced by ionomycin (2 μM) in the presence of 1.3 mM $CaCl_2$, both in naive and L-AP4-treated synaptosomes. *C*, release facilitation in L-AP4-treated synaptosomes at different ionomycin concentrations. The release induced by each ionomycin concentration in naive synaptosomes was taken as control, and the data on the effect of ionomycin concentration on release facilitation are presented as compared with the control. *D*, pharmacology of the L-AP4-induced release potentiation. The ionomycin (2 μM)-induced release was determined in L-AP4-treated synaptosomes in the presence of drugs added at different times prior to iomomycin: the group III mGlu receptor antagonist CPPG (100 μM, 15 min), the mGluR5 antagonist 2-methyl-6(phenylethynyl)pyridine (*MPEP*) (10 μM, 35 min), the mGluR1 antagonist CPCCOEt (1 mM, 35 min), the group II mGluR antagonist LY-341495 (20 nM, 35 min), pertussis toxin (1.5 μg/ml, 2 h), the active PLC inhibitor U-73122 (2 μM, 30 min), the inactive PLC inhibitor U-73343 (2 μM, 30 min), PKA inhibitor H-89 (10 μM, 30 min), adenylyl cyclase inhibitor SQ-22536 (10 μM, 30 min), the PKC inhibitor calphostin C (0.1 μM, 30 min), and bisindolylmaleimide (1 μM, 30 min). The release induced by ionomycin (2 μM) in naive synaptosomes was taken as control and the data on the effect of the different treatments are shown as compared with the control. The results are the mean ± S.E. ($n = 6–8$). *NS*, $p > 0.05$; ***, $p < 0.001$ (unpaired *t* test) when compared with control values.

KCl evokes maximal glutamate release, this stimulation condition establishes a ceiling above that no facilitation can be observed. Thus, we used lower KCl concentrations to make release facilitation possible. Glutamate release in naive synaptosomes stimulated with 5 mM KCl (0.9 ± 0.11 nmol, $n = 6$, Fig 1, *I* and *J*) was reduced to 45.8 ± 4% of the control value by the initial addition of L-AP4 ($n = 6$, $p < 0.05$). Interestingly, in nerve terminals previously exposed to L-AP4 the glutamate release evoked by 5 mM KCl was potentiated (165.8 ± 6.4% of control, $n = 6$, $p < 0.01$). Furthermore, a second addition of L-AP4 failed to inhibit the release of glutamate (90.5 ± 3.1% of control, $n = 6$, $p > 0.05$) and thus, exposure of synaptosomes to L-AP4 promoted a new response that augmented the release and counteracted its inhibition due to diminished Ca^{2+} influx.

Release Facilitation—As release inhibition is mediated by impaired Ca^{2+} channel activity, release facilitation was separated from its inhibition by inducing release with the Ca^{2+} ionophore ionomycin, which inserts into the membrane and delivers Ca^{2+} to the release machinery independently of Ca^{2+} channel activity (25). We first performed a time course to determine the time of L-AP4 pre-treatment needed to obtain optimal release potentiation. Although a remarkable increase in release was obtained after a 4-min incubation, maximal potentiation required 10 min of treatment with L-AP4 (1 mM) and this time was adopted as the standard (Fig. 2*A*). The ionomycin-induced release in naive synaptosomes was 0.65 ± 0.01 nmol of Glu/mg of protein ($n = 26$), and this ionomycin-induced release was increased to 1.1 ± 0.05 nmol of Glu/mg of protein in synaptosomes exposed to L-AP4 for 10 min ($n = 26$, $p < 0.001$, Fig. 2*B*). L-AP4-mediated potentiation

FIGURE 1. **L-AP4 treatment unmasks release potentiation by mGlu7 receptors.** Synaptosomes were fixed onto polylysine-coated coverslips and double stained for immunocytochemistry with antisera against mGlu7a (*A*), 4a (*B*), and 8a (*C*) receptors and the vesicular marker synaptophysin. *Scale bar*, 2 μm. *D*, mGluR7a, -4a, and -8a expression in synaptophysin-containing nerve terminals. Ca^{2+}-dependent release of glutamate (*E*, *F*, *I*, and *J*) and changes in the cytoplasmic free Ca^{2+} concentration, $[Ca^{2+}]_c$ (*G* and *H*) evoked by 30 mM (*E–H*) and 5 mM KCl (*I* and *J*) in naive and L-AP4-treated nerve terminals. Synaptosomes were exposed to 1 mM L-AP4 for 10 min and then washed, centrifuged, and resuspended to remove the agonist (*L-AP4-treated*). Naive synaptosomes were treated in the same way but in the absence of L-AP4. *F* shows summarized data on release inhibition by L-AP4 (*red*) as compared with their respective control. The 30 mM KCl-induced release in the absence of L-AP4 either in naive or L-AP4-treated synaptosomes was taken as control. *G*, the KCl-induced rise in $[Ca^{2+}]_c$ was reduced by L-AP4 both in naive and L-AP4-treated synaptosomes. *Dashed lines* show the $[Ca^{2+}]_c$ in the absence of L-AP4 (*control*). The $[Ca^{2+}]_c$ reached 1 min after depolarization was taken as control both in naive and L-AP4-treated nerve terminals. *H* shows the L-AP4 effect on $[Ca^{2+}]_c$ as a fraction of control values. *J*, summarized data on release inhibition by L-AP4 (*red*) as compared with their respective control. The 5 mM KCl-induced release in the absence of L-AP4 either in naive or L-AP4-treated synaptosomes were taken as control. In release facilitation experiments (*green*), 5 mM KCl-induced release in naive synaptosomes was taken as control and data are presented as compared with control. Results are the mean ± S.E. ($n = 8$). *NS*, $p > 0.05$; *, $p < 0.05$; **, $p < 0.01$; ***, $p < 0.001$ (unpaired *t* test) when compared with corresponding control values.

was only observed at submaximal ionomycin concentrations of 2 to 6 μM (Fig. 2*C*), suggesting that the releasable vesicle pool disappeared at higher ionomycin concentrations. Thus, at 15 μM ionomycin no release potentiation was observed (99.9 ± 1.6%, $n = 5$, $p > 0.05$). We set out to characterize the L-AP4-mediated modulation of release pharmacologically. Release potentiation was prevented by the group III mGlu receptors antagonist (*R*,*S*)-α-cyclopropyl-4-phosphono-phenylglycine (CPPG, 100.4 ± 5.3% of control, $n = 8$, $p > 0.05$, Fig. 2*D*). Neither the mGluR5 antagonist 2-methyl-6-(phenylethynyl)pyridine nor the mGluR1 antagonist 7-(hydroxyimino)cyclopropa[*b*]chromen-1a-carboxylate ethyl ester (CPCCOEt) altered L-AP4-mediated release facilitation (167.0 ± 6.2%, $n = 4$, $p < 0.001$ and 168.1 ± 1.5%, $n = 4$, $p < 0.001$, respectively). The group II mGluR antagonist LY-341495 was also without effect on the L-AP4-mediated facilitation (166.5 ± 3.4%, $n = 4$, $p < 0.001$). Pertussis toxin had no effect on release facilitation (163.5 ± 3.5%, $n = 8$, $p < 0.001$), indicating that G_i/G_o proteins were not involved. In parallel experiments, PTX prevented inhibition of the release by the $GABA_B$ receptor agonist baclofen (32.2 ± 5.7%, $n = 3$, and 4.7 ± 3.1%, $n = 3$, of release inhibition), in the absence and presence of pertussis toxin, respectively. Thus, indicating the inactivation of the G protein by the toxin. Interestingly, the phospholipase C (PLC) inhibitor U-73122 abolished this response (100.3 ± 0.9%, $n = 7$, $p > 0.05$), whereas its inactive analogue U-73343 had no such effect (164.1 ± 8.2%, $n = 8$, $p < 0.001$). Furthermore, neither the cAMP-dependent protein kinase (PKA), inhibitor H-89 (173.0 ± 3.1%, $n = 8$, $p < 0.001$), or the adenylyl cyclase inhibitor (SQ-22536) (168.5 ± 4.0%, $n = 8$, $p < 0.001$) altered release potentiation. We also tested whether release facilitation was sensitive to protein kinase C inhibitors and found that bisindolylmaleimide, the specific inhibitor of protein kinase C, which prevents ATP binding, did not affect the response (168.2 ± 4.3%, $n = 6$, $p < 0.001$). By contrast, calphostin C abolished L-AP4-mediated release potentiation (106.9 ± 3.2%, $n = 6$, $p > 0.05$: Fig. 2*D*). As calphostin C acts at the diacylglycerol binding site, and therefore it also inhibits, nonkinase DAG-binding proteins such as munc13s (26), these data suggested the involvement of this latter protein in the L-AP4-mediated release potentiation.

As prolonged exposure to L-AP4 potentiated counterbalancing release inhibition despite impaired Ca^{2+} influx, pharmacological blockage of the facilitating pathway should permit the recovery of release inhibition in response to a second addition of L-AP4. Inhibition of release by a second addition of L-AP4 was still evident in nerve terminals that were pre-exposed to L-AP4 but in the presence of the active PLC inhibitor U-73122 (61.5 ± 4.9% of control, $n = 5$, $p < 0.001$: Fig. 3, *A* and *B*). By contrast, exposure to L-AP4 in the presence of the inactive PLC inhibitor U-73343 results in the lack of release inhibition by a second addition of the agonist (99.2 ± 1.9% of control, $n = 5$, $p > 0.05$). Because release facilitation counterbalances release inhibition observed upon 30 mM KCl depolarization, altering the extent of release facilitation should also affect the extent of release inhibition. Exposing nerve terminals to different L-AP4 concentrations (0.5–1.0 mM) would be expected to produce graded release facilitation and hence, these conditions were

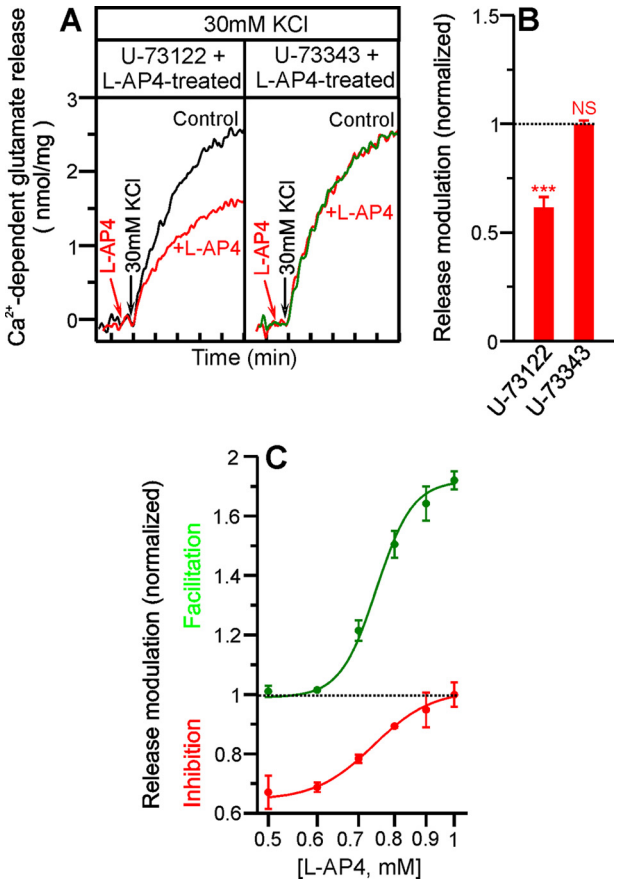

FIGURE 3. **Release modulation by mGlu7 receptors is a balance between inhibition and facilitation.** Pharmacological blockage of PLC not only prevents L-AP4-induced release potentiation but also allows recovery of release inhibition by a second addition of L-AP4. Synaptosomes were exposed to 1 mM L-AP4 for 10 min in the presence of the PLC inhibitor, U-73122, or its inactive analogue, U-73343 (*A*). After washing, centrifuging, and resuspending, the synaptosomes were tested for release inhibition by a second addition of L-AP4 prior to depolarization with 30 mM KCl. *B*, diagrams show summarized data on release inhibition by a second addition of L-AP4. The release induced by 30 mM KCl in L-AP4-treated nerve terminals, but in the absence of a second addition of L-AP4, was taken as control. *C*, lowering the L-AP4 concentration of treated synaptosomes decreases the extent of release facilitation and allows the recovery of release inhibition by a second addition of L-AP4. Synaptosomes exposed to L-AP4 (0.5–1 mM) for 10 min were used to test release facilitation by estimating the ionomycin-induced release and to test release inhibition by depolarizing nerve terminals with 30 mM KCl after a second addition of L-AP4 (1 mM). In release facilitation experiments (*green*), the release induced by 2 μM ionomycin in naive synaptosomes was taken as control. In release inhibition experiments (*red*), the release induced by 30 mM KCl in naive synaptosomes was taken as control. Data on the effect of different L-AP4 concentration pre-treatments both in release facilitation and inhibition are presented as compared with control. The data represent the mean ± S.E. ($n = 5$). *NS*, $p > 0.05$; ***, $p < 0.001$ (unpaired *t* test) when compared with corresponding control values.

used to test for the potentiation of ionomycin-induced release or for the inhibition of KCl-evoked release. At 1 mM L-AP4, maximal release potentiation was observed (172.0±.3.0%, $n = 5$, $p < 0.001$), whereas this treatment completely abolished release inhibition in response to a second addition of the agonist (100.1 ± 4.1%, $n = 5$, $p > 0.05$: Fig. 3*C*). However, in synaptosomes that had been treated with lower L-AP4 concentrations, the facilitation of ionomycin-induced release decreased and a progressive recovery of release inhibition was observed. Thus, at 0.5 mM L-AP4, release potentiation was abolished (101.0 ± 1.9%, $n = 5$, $p > 0.05$), whereas release inhibition was

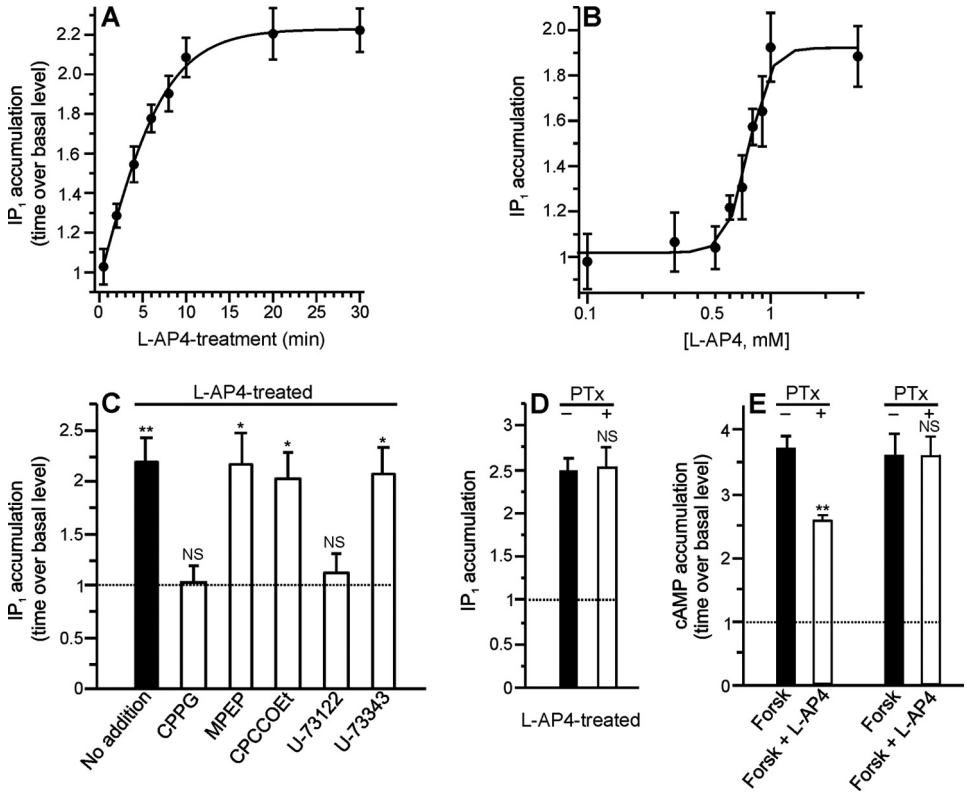

FIGURE 4. **L-AP4 enhances IP_1 accumulation.** *A*, time course of L-AP4 treatment on IP_1 accumulation. Synaptosomes were exposed to L-AP4 (1 mM) for the indicated times and processed as indicated under "Experimental Procedures" to estimate IP_1 accumulation. *B*, concentration-response curve of L-AP4-induced IP_1 accumulation. *C*, pharmacology of L-AP4-induced IP_1 accumulation. Synaptosomes were incubated with L-AP4 for 20 min. Drugs were present for the times indicated: CPPG (100 μM) 35 min; 2-methyl-6-(phenylethynyl)pyridine (*MPEP*) (10 μM) 35 min; CPCCOEt (1 mM) 35 min; U-73122 (2 μM) 40 min; and U-73343 (2 μM) 40 min. The results are presented as the fold-increase over basal levels of IP_1 in naive nerve terminals (6.4 $\pm$ 0.05 pmol). *D*, sensitivity of L-AP4-induced IP_1 accumulation to pertussis toxin. Synaptosomes were incubated with PTX (1.5 μg/ml, 2 h) and then stimulated with 1 mM L-AP4 for 20 min. *E*, sensitivity of the L-AP4-induced decrease of forskolin-stimulated cAMP levels to PTX. Synaptosomes were incubated with PTX (1.5 μg/ml, 2 h) and then stimulated with 100 μM forskolin for 15 min, followed by 1 mM L-AP4 for another 5 min. Results are presented as the fold-increase over basal cAMP levels in naive synaptosomes (19.2 $\pm$ 0.7 pmol). The data represent the mean $\pm$ S.E. ($n = 4-8$). *NS*, $p > 0.05$; *, $p < 0.05$; **, $p < 0.01$ (unpaired *t* test), when compared with the basal levels (*panel C*). In experiments with PTX the data were compared with those in the absence of PTX (*panels D* and *E*).

maximal (67.1 $\pm$ 5.6% of control, $n = 5$, $p < 0.001$). These results indicate that the extent of release facilitation by mGlu7 receptors dynamically controls the extent of release inhibition.

Phosphatidylinositol Hydrolysis—Because L-AP4-mediated potentiation of release is suppressed by PLC inhibitors, we tested whether phosphatidylinositol hydrolysis and subsequent formation of DAG and inositol trisphosphate could be involved in this process. IP_1 accumulation can be measured instead of inositol trisphosphate to monitor the activity of GPCRs linked to PLC in which LiCl inhibits inositol monophosphatase (27). A time course study showed that a 10–20-min pre-exposure to L-AP4 is required to obtain maximal IP_1 accumulation (Fig. 4*A*). We also found that prolonged incubations with L-AP4 enhanced IP_1 accumulation in a dose-dependent manner, although high L-AP4 concentrations were required (Fig. 4*B*). Neither the mGlu5 receptor antagonist, 2-methyl-6(phenylethynyl)pyridine (217.2 $\pm$ 30.7%, $n = 4$, $p < 0.05$), nor the mGlu1 receptor antagonist, CPCCOEt (203.1 $\pm$ 26.0%, $n = 4$, $p < 0.05$), prevented this response, excluding group I mGlu receptor activation under these conditions. However, the group III mGlu receptors antagonist CPPG did abolish this response (101.9 $\pm$ 17.0%, $n = 8$, $p > 0.05$). Accordingly, the PLC inhibitor U-73122 also blocked the response (113.4 $\pm$ 18.7%, $n = 4$, $p > 0.05$), whereas its inactive analogue U-73343 did not (207.7 $\pm$ 24.8%, $n = 4$, $p < 0.05$) (Fig. 4*C*). In keeping with release experiments, preincubation with pertussis toxin did not modify the accumulation of IP_1 elicited by L-AP4 (248.5 $\pm$ 12.7%, $n = 4$, $p < 0.05$ and 250.7 $\pm$ 24.8%, $n = 4$, $p < 0.05$ in the presence and absence of PTX, respectively, Fig. 4*D*). Moreover, as a positive control we showed that the increase in basal cAMP levels induced by the adenylyl cyclase activator forskolin (373.5 $\pm$ 15.3%, $n = 4$) was significantly reduced by L-AP4 (256.6 $\pm$ 9.9%, $n = 4$, $p < 0.01$), and that preincubation with PTX abolished this response (360.0 $\pm$ 30.1%, $n = 4$, $p > 0.05$, Fig. 4*E*).

mGlu7 Receptor Translocates Munc13-1 Protein—L-AP4-mediated release facilitation was insensitive to the PKC inhibitor bisindolylmaleimide but was blocked by calphostin C, which also inhibits non-kinase DAG-binding proteins such as munc13-1. The active zone protein munc13-1 is a phorbol ester receptor essential for synaptic vesicle priming involved in neurotransmitter release potentiation (16, 17, 27). Munc13-1 is distributed in two biochemically distinguishable soluble and insoluble pools (16, 28, 29). As diacylglycerol and phorbol esters increase the association of munc13-1 with the plasma membrane (26, 30), we tested whether mGlu7 receptor activation alters the subcellular distribution of munc13-1 between the soluble and particulate fractions derived from synaptosomes after hypoosmotic shock. The soluble fraction was characterized by a high lactic dehydrogenase content (80.6 $\pm$ 1.5%, $n = 6$, Fig. 5*B*), moderate content of a vesicular marker (vGluT1 35.6 $\pm$ 2.3%, $n = 6$), and minor amounts of the plasma membrane markers acetylcholinesterase (AChase: 11.2 $\pm$ 1.4%, $n = 6$) or Na^+,K^+-ATPase (0.1 $\pm$ 5%, $n = 6$: Fig. 5*B*). By contrast, the particulate fraction had little LDH (19.4 $\pm$ 1.5, $n = 6$), whereas vGluT1 (64.4 $\pm$ 2.3%, $n = 6$), AChase (88.8 $\pm$ 1.4%, $n = 6$), and ATPase (99.9 $\pm$ 5%, $n = 6$) were enriched (Fig. 5*B*). The munc13-1 content in the soluble and particulate fraction were determined in Western blots (Fig. 5*A*) that were quantified by densitometry (Fig. 5*C*). In naive nerve terminals, the soluble to particulate (S/P) munc13-1 content ratio was 0.30 $\pm$ 0.08 ($n = 6$) and this value fell significantly following exposure to L-AP4 (0.05 $\pm$ 0.01, $p < 0.01$, $n = 6$), indicating that munc13-1 translocate from the soluble to par-

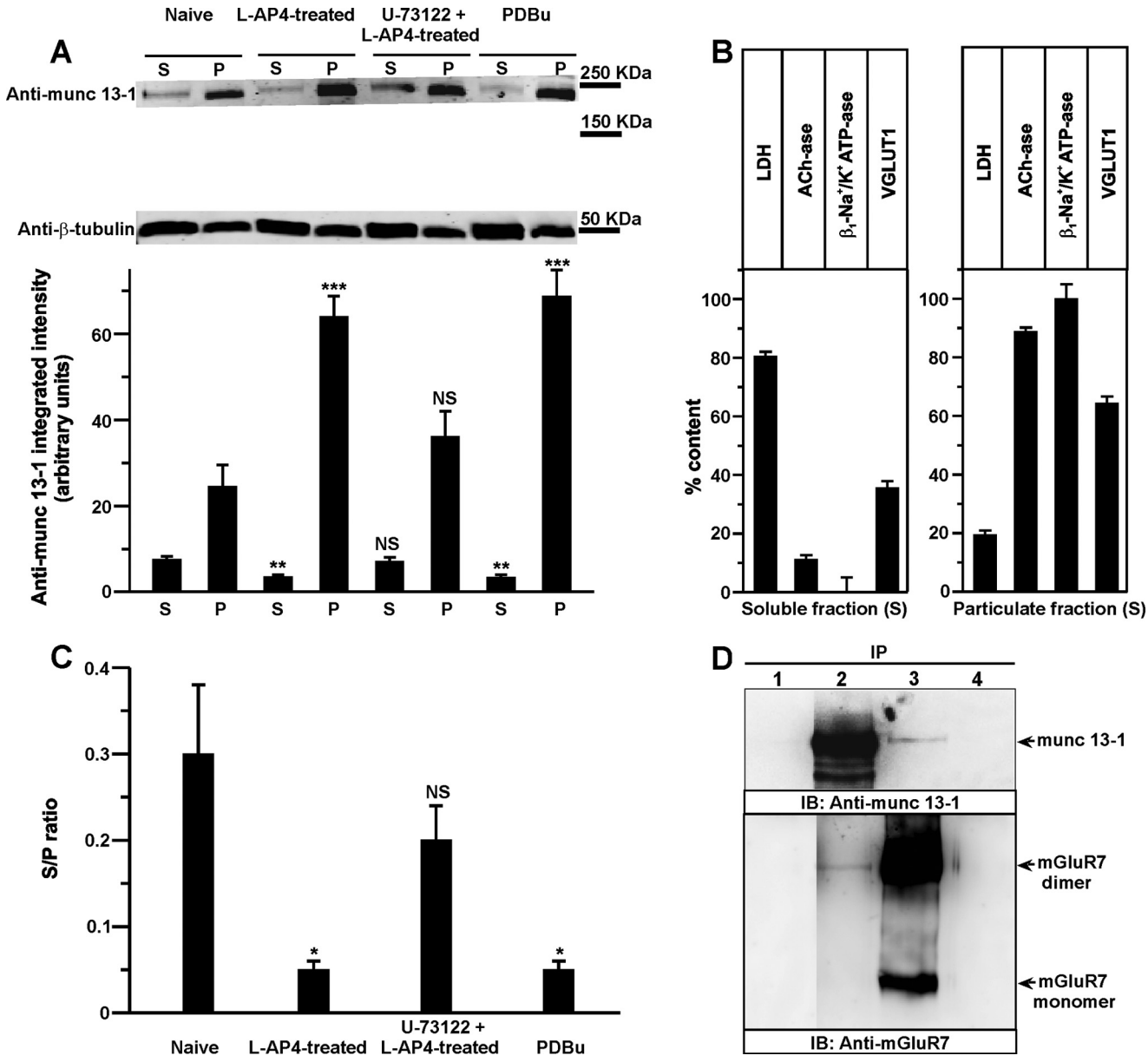

FIGURE 5. **mGlu7 receptors translocate munc13-1 protein.** *A*, munc13-1 protein content in soluble and particulate fractions of naive and L-AP4-treated synaptosomes, and in L-AP4-treated synaptosomes in the presence of the PLC inhibitor U-73122. Munc13-1 protein translocation was also determined in synaptosomes treated with phorbol 12,13-dibutyrate (*PDBu*) (1 μM, 2 min). Diagrams show the quantification of the munc13-1 content in soluble and particulate fractions from synaptosomes treated under the aforementioned conditions. *B*, characterization of soluble and particulate fractions are based on protein content. The relative content of acetylcholinesterase (*AChase*) and LDH enzymatic (determined fluorometrically), and vGlut1 and Na^+,K^+-ATPase (determined in Western blot) was estimated in each fraction, and the sum of the soluble and particulate fraction values taken as 100%. *C*, the ratio between soluble and particulate munc13-1 fractions were calculated in each experiment. Data represent the mean ± S.E. ($n = 6$). *NS*, $p > 0.05$; *, $p < 0.05$; **, $p < 0.01$; ***, $p < 0.001$ (unpaired *t* test), when compared with either the soluble or particulate fractions, or the *S/P* ratio from naive synaptosomes. *D*, co-immunoprecipitation of mGlu7 receptors and munc13-1 from the cerebrocortical synaptosomes. Solubilized extracts were subjected to immunoprecipitation (*IP*) with rabbit anti-FLAG antibody (5 μg, *lane 1*), rabbit anti-munc13-1 polyclonal antiserum (5 μg, *lane 2*), rabbit anti-mGlu7 receptor polyclonal antiserum (5 μg, *lane 3*), and mouse anti-FLAG antibody (5 μg, *lane 4*). Extracts (*Crude*) and immunoprecipitates were analyzed in Western blots probed with a rabbit anti-mGlu7 receptor polyclonal antiserum (2.5 μg/ml) or a rabbit anti-munc13-1 polyclonal antiserum (1 μg/ml). Horseradish peroxidase-conjugated anti-rabbit IgG TrueBlot (1:1000) was used as a secondary antibody to avoid IgG cross-reactivity and the immunoreactive bands were visualized by chemiluminescence. *IB*, immunoblot.

ticulate fraction. This shift was prevented by U-73122 (0.20 ± 0.04, $p > 0.05$, $n = 6$), whereas phorbol 12,13-dibutyrate also promoted munc13-1 translocation (S/P ratio, 0.05 ± 0.01, $p < 0.01$, $n = 6$). Overall, these data indicate that the mGlu7 receptor provokes translocation of munc13-1 protein from soluble to a particulate fraction within nerve terminals.

Given that the mGlu7 receptor and munc13-1 proteins both localize at the presynaptic active zone (1, 31), co-immunoprecipitation experiments were performed using P_2 synaptosomes. The anti-munc13-1 antibody immunoprecipitated a band of around 200 kDa that appeared to correspond to the munc13-1 protein (29) (Fig. 5*D*), whereas the anti-mGlu7 receptor antibody was able to immunoprecipitate a band of around 200 kDa that corresponded to the mGlu7 receptor dimer (Fig. 5*D*), as demonstrated previously (23). Significantly, whereas the anti-munc13-1 antibody was able to co-immunoprecipitate the

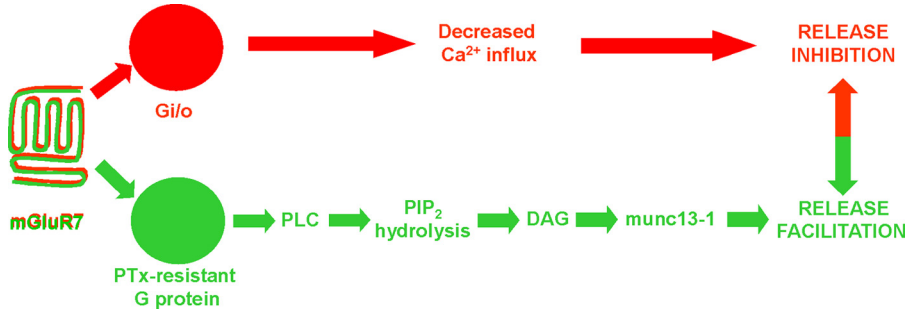

FIGURE 6. **Dual modulation of glutamate release by mGlu7 receptors.** Scheme illustrating the putative signaling pathways activated by mGluR7. Exposure to agonist L-AP4 (1 mM, 30 s) initiates a signaling cascade that activates the pertussis toxin-sensitive G protein ($G_{i/o}$), resulting in the reduction of evoked Ca^{2+} influx and glutamate release. Longer exposures to agonist (1 mM, 10 min) results in the potentiation of glutamate release. Release potentiation involves a PTX-resistant G protein that activates PLC, increasing phosphatidylinositol (4,5)-bisphosphate (*PIP_2*) hydrolysis and promoting DAG-dependent translocation of the munc13-1 protein.

mGlu7 receptor, the anti-mGlu7 receptor antibody could also co-immunoprecipitate munc13-1 (Fig. 5*D*). These bands did not appear when an irrelevant rabbit or mouse IgG were used for immunoprecipitation (Fig. 5*D*, *lanes 1* and *4*, respectively), showing the specificity of the reaction. These results suggest that the mGlu7 receptor and munc13-1 might assemble into stable protein-protein complexes in the rat cortex that survive the solubilization and co-immunoprecipitation conditions employed. The stability of these oligomeric complexes indicates that they might be physiologically relevant *in vivo*.

DISCUSSION

It is well established that metabotropic glutamate receptor 7 inhibits glutamate release by decreasing presynaptic Ca^{2+} influx through voltage-dependent calcium channels. Using a preparation of nerve terminals from the cerebral cortex, we found that in addition to mediating release inhibition, mGlu7 receptor also activates signaling pathways that potentiate release. Release potentiation requires at least a 10-min exposure to a receptor agonist and once the mechanism of release potentiation is established, it occludes the release inhibition produced by a second addition of the agonist. In contrast to the PTX-sensitive G protein that impedes Ca^{2+} channel activity in mGlu7 receptor-dependent inhibition of release, the mGlu7 receptor response that potentiates release involves a PTX-resistant G protein that activates PLC, increasing phosphatidylinositol hydrolysis and promoting DAG-dependent translocation of the munc13-1 protein.

In addition to the well established inhibition of voltage-dependent Ca^{2+} channels (5, 32–34) and adenylyl cyclase (5), mGlu7 receptor couples to other signaling pathways such as those that activate GIRK channels (35) or PLC (7). However, the physiological relevance of these signaling mechanisms in synaptic glutamate release modulation remain largely unknown. Thus, mGlu7 receptor-mediated GIRK channel activation is limited to heterologous expression systems and whether this signaling occurs at synaptic sites remains to be shown. When ectopic mGlu7 receptors are expressed in cerebellar granule cells, somatic Ca^{2+} currents are inhibited via PLC activation (7), although the relevance of this signaling at synaptic sites remains unclear. Our finding that synaptic mGlu7 receptor activates a PLC-dependent pathway that leads to release potentiation is consistent with previous work showing that presynaptic PLC is involved in synaptic release potentiation in cultured hippocampal neurons (18). In this study, release potentiation induced by high frequency stimulation (HFS) was blocked by the active PLC inhibitor, U-73122 (18). As PLC is a Ca^{2+}-dependent enzyme, it was proposed that PLC was activated by the increase in presynaptic Ca^{2+} influx induced by HFS. Our data suggest that in addition to Ca^{2+}, presynaptic PLC is also activated by PTX-insensitive G proteins. Nevertheless, high frequency stimulation increases synaptic release of glutamate to levels sufficient to activate mGlu7 receptors (19), despite the low affinity reported for this receptor for glutamate (36). The identity of the PLC isoform involved in L-AP4-mediated release potentiation at cerebrocortical synapses remains unclear. At least 13 PLC isoforms have been identified in mammals that belong to six families that are designated: -β, -γ, -δ, -ϵ, -ζ, and PLC-η, and some of which are abundantly expressed in the brain (PLC-β, -γ, and -η) (14, 37, 38). Although all PLCs catalyze the hydrolysis of phosphatidylinositol (4,5)-bisphosphate, thereby generating DAG and inositol trisphosphate, the presence of distinct regulatory domains in PLC isoforms renders them susceptible to different modes of activation. Thus, all PLCs require Ca^{2+} with the δ-, ζ-, and η-type being the most sensitive to this cation. In addition, $G\alpha_q$ proteins activate PLCβ but not the other isozymes, whereas $G\beta\gamma$ can activate PLCβ, -ϵ, and -η (14, 39). Thus, at least three PLCs can be activated by GPCRs.

Recent reports have shown that mGlu7 receptors bidirectionally control plasticity at hippocampal synapse (19). In naive slices, mGlu7 receptor activation during HFS generates long term depression, at synapses between mossy fibers and stratum lucidum interneurons due to a persistent decrease in glutamate release. However, the exposure of hippocampal slices to agonist L-AP4 internalizes mGlu7 receptors, unmasking the ability of these synapses to undergo presynaptic potentiation in response to the same HFS that induced long term depression in naive slices. L-AP4-mediated potentiation of release found at cerebrocortical boutons has some similarities with HFS-induced long term potentiation, and of mossy fiber synapses found in L-AP4-treated hippocampal slices (40). At both synapses release potentiation requires prolonged exposure to L-AP4 and it occurs despite the persistent reduction in Ca^{2+} influx. However, whereas potentiation at MF-SLIN synapses is prevented by either the adenylyl cyclase inhibitor DDOA or the PKA inhibitor H-89, L-AP4-mediated potentiation at cerebrocortical nerve terminals is insensitive to these compounds, although it is blocked by U-73122.

The bidirectional control of glutamate release raises the question whether there is a single population of nerve terminals in which L-AP4 has a dual role in release modulation or whether there are two populations of regulated nerve terminals, one that

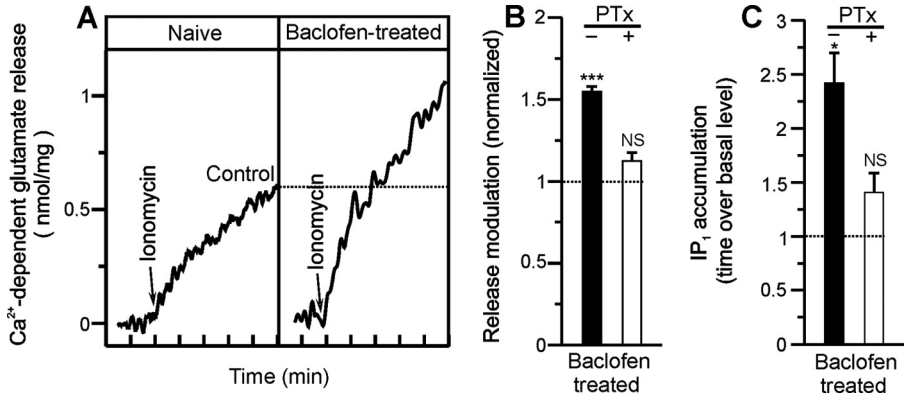

FIGURE 7. **$GABA_B$ receptors also potentiate glutamate release.** *A*, glutamate release induced by ionomycin (2 μM) in the presence of 1.3 mM $CaCl_2$, both in naive and baclofen-treated synaptosomes (20 μM, 10 min). *B*, the ionomycin (2 μM)-induced release was determined in baclofen-treated synaptosomes in the absence and presence of pertussis toxin (1.5 μg/ml, 2 h). *C*, sensitivity of baclofen-induced IP_1 accumulation to pertussis toxin. IP_1 accumulation was determined in baclofen-treated synaptosomes in the absence and presence of PTX (1.5 μg/ml, 2 h). The data represent the mean ± S.E. ($n = 4$). *NS*, $p > 0.05$; *, $p < 0.05$; ***, $p < 0.001$ (unpaired *t* test) when compared with the basal levels.

is inhibited and another that is potentiated by L-AP4 with different kinetics. The finding, however, that a second addition of L-AP4 fails to inhibit release (Fig. 1*E*) suggests that L-AP4 both inhibits and facilitates glutamate release in the same population of nerve terminals. Otherwise, a second pulse of L-AP4 would reduce glutamate release, as it inhibits Ca^{2+} influx (Fig. 1*G*).

Because mGlu7 receptors immunoprecipitated the presynaptic active zone protein munc13-1, which is thought to be required for the DAG-dependent potentiation of synaptic transmission, the two proteins appear to assemble into the same stable protein complexes (either through a direct or indirect interaction). RIM1α, an active zone molecule required for long term adenylate cyclase/PKA-dependent potentiation (41, 42) was recently shown to associate with mGlu7 receptors. Moreover, L-AP4 impaired the co-precipitation of mGlu7b receptor-RIM1α suggesting that the two proteins exist within the same molecular complex and that this interaction can be disrupted by receptor activation/internalization. This association would provide a potential molecular mechanism to explain how mGlu7 receptor internalization primes mossy fiber-stratum lucidum interneurons synapses to become long term potentiation competent (40). Interestingly, it was shown that munc13-1 (which is essential for priming synaptic vesicles to a fusion competent state and restricting transmitter release to the active zone) interact with RIM1α (a Rab3A-interacting protein), and that this interaction serves to recruit munc13-1 to the active zone (43). All these data suggest that the mGlu7 receptor complexes with proteins are involved in receptor-mediated signaling relevant for modulating glutamate release.

In summary, we have described a dual role of the mGlu7 receptor in control of glutamate release as this receptor can either inhibit or enhance this process (see Fig. 6). It is likely that the negative feedback control of release exerted by the inhibitory branch of the mGlu7 receptor signaling pathway may help prevent the accumulation of glutamate at synapses and the neurotoxic effects of this neurotransmitter. However, the physiological relevance of the new signaling involved in release facilitation is still not known. Because the mGlu7 receptor is less efficiently coupled to release facilitation than to the release inhibition pathway, as evident by the prolonged exposure to agonist required for activation (at least 10 min), it seems that the major function of the receptor would appear to be to provide presynaptic inhibition control. This is consistent with data showing that the lack of functional mGlu7 receptor leads to a convulsive phenotype due to excessive glutamate release (44, 45). A possible role for L-AP4-mediated release potentiation would be to preserve homeostasis by preventing synapses in saturating states of depression from accumulating glutamate. One important question is whether this dual control of glutamate release also applies to other presynaptic receptors that inhibit release. We have recently reported that the mGlu7 receptor is coexpressed with other presynaptic receptors that inhibit neurotransmitter release, such as adenosine A_1 and $GABA_B$ receptors (46, 47). We found that exposure of nerve terminals to the $GABA_B$ receptor agonist baclofen enhanced glutamate release as well as IP_1 accumulation, although in this case, a G protein sensitive to pertussis toxin was involved in both responses (Fig. 7, *A–C*). These data indicate that the bidirectional control of glutamate release may be a more general mechanism not restricted to mGlu7.

Acknowledgements—We thank Dr. R. Shigemoto for providing mGluR4a, mGluR7a, and mGluR8a antibodies. We also thank Hélène Orcel for technical assistance in performing second messenger measurements. We also thank the Plateforme de Pharmacologie-Criblage of Montpellier and the Region Languedoc-Rousillon.

REFERENCES

1. Shigemoto, R., Kulik, A., Roberts, J. D., Ohishi, H., Nusser, Z., Kaneko, T., and Somogyi, P. (1996) *Nature* **381,** 523–525
2. Forsythe, I. D., and Clements, J. D. (1990) *J. Physiol.* **429,** 1–16
3. Gereau, R. W., 4th, and Conn, P. J. (1995) *J. Neurosci.* **15,** 6879–6889
4. Herrero, I., Vazquez, E., Miras-Portugal, M. T., and Sánchez-Prieto, J. (1996) *Eur. J. Neurosci.* **8,** 700–709
5. Millán, C., Luján, R., Shigemoto, R., and Sánchez-Prieto, J. (2002) *J. Biol. Chem.* **277,** 14092–14101
6. Blackmer, T., Larsen, E. C., Bartleson, C., Kowalchyk, J. A., Yoon, E. J., Preininger, A. M., Alford, S., Hamm, H. E., and Martin, T. F. (2005) *Nat. Neurosci.* **8,** 421–425
7. Perroy, J., Prezeau, L., De Waard, M., Shigemoto, R., Bockaert, J., and Fagni, L. (2000) *J. Neurosci.* **20,** 7896–7904
8. Herrero, I., Miras-Portugal, M. T., and Sánchez-Prieto, J. (1992) *J. Neurochem.* **59,** 1574–1577
9. Parfitt, K. D., and Madison, D. V. (1993) *J. Physiol.* **471,** 245–268
10. Stea, A., Soong, T. W., and Snutch, T. P. (1995) *Neuron* **15,** 929–940
11. Zhang, Y. H., Kenyon, J. L., and Nicol, G. D. (2001) *J. Neurophysiol.* **85,** 362–373
12. Stevens, C. F., and Sullivan, J. M. (1998) *Neuron* **21,** 885–893
13. Wu, X. S., and Wu, L. G. (2001) *J. Neurosci.* **21,** 7928–7936
14. Rhee, S. G. (2001) *Annu. Rev. Biochem.* **70,** 281–312
15. Wierda, K. D., Toonen, R. F., de Wit, H., Brussaard, A. B., and Verhage, M. (2007) *Neuron* **54,** 275–290

16. Betz, A., Ashery, U., Rickmann, M., Augustin, I., Neher, E., Südhof, T. C., Rettig, J., and Brose, N. (1998) *Neuron* **21,** 123–136
17. Rhee, J. S., Betz, A., Pyott, S., Reim, K., Varoqueaux, F., Augustin, I., Hesse, D., Südhof, T. C., Takahashi, M., Rosenmund, C., and Brose, N. (2002) *Cell* **108,** 121–133
18. Rosenmund, C., Sigler, A., Augustin, I., Reim, K., Brose, N., and Rhee, J. S. (2002) *Neuron* **33,** 411–424
19. Pelkey, K. A., Lavezzari, G., Racca, C., Roche, K. W., and McBain, C. J. (2005) *Neuron* **46,** 89–102
20. Herrero, I., Castro, E., Miras-Portugal, M. T., and Sánchez-Prieto, J. (1991) *Neurosci. Lett.* **126,** 41–44
21. Grynkiewicz, G., Poenie, M., and Tsien, R. Y. (1985) *J. Biol. Chem.* **260,** 3440–3450
22. Trinquet, E., Fink, M., Bazin, H., Grillet, F., Maurin, F., Bourrier, E., Ansanay, H., Leroy, C., Michaud, A., Durroux, T., Maurel, D., Malhaire, F., Goudet, C., Pin, J. P., Naval, M., Hernout, O., Chrétien, F., Chapleur, Y., and Mathis, G. (2006) *Anal. Biochem.* **358,** 126–135
23. Shigemoto, R., Kinoshita, A., Wada, E., Nomura, S., Ohishi, H., Takada, M., Flor, P. J., Neki, A., Abe, T., Nakanishi, S., and Mizuno, N. (1997) *J. Neurosci.* **17,** 7503–7522
24. Pelkey, K. A., Yuan, X., Lavezzari, G., Roche, K. W., and McBain, C. J. (2007) *Neuropharmacology* **52,** 108–117
25. Jovanovic, J. N., Czernik, A. J., Fienberg, A. A., Greengard, P., and Sihra, T. S. (2000) *Nat. Neurosci.* **3,** 323–329
26. Brose, N., and Rosenmund, C. (2002) *J. Cell Sci.* **115,** 4399–4411
27. Bauer, C. S., Woolley, R. J., Teschemacher, A. G., and Seward, E. P. (2007) *J. Neurosci.* **27,** 212–219
28. Brose, N., Hofmann, K., Hata, Y., and Südhof, T. C. (1995) *J. Biol. Chem.* **270,** 25273–25280
29. Kalla, S., Stern, M., Basu, J., Varoqueaux, F., Reim, K., Rosenmund, C., Ziv, N. E., and Brose, N. (2006) *J. Neurosci.* **26,** 13054–13066
30. Ashery, U., Varoqueaux, F., Voets, T., Betz, A., Thakur, P., Koch, H., Neher, E., Brose, N., and Rettig, J. (2000) *EMBO J.* **19,** 3586–3596
31. Rosenmund, C., Rettig, J., and Brose, N. (2003) *Curr. Opin. Neurobiol.* **13,** 509–519
32. Millán, C., Luján, R., Shigemoto, R., and Sánchez-Prieto, J. (2002) *J. Biol. Chem.* **277,** 47796–47803
33. Millán, C., Castro, E., Torres, M., Shigemoto, R., and Sánchez-Prieto, J. (2003) *J. Biol. Chem.* **278,** 23955–23962
34. Pelkey, K. A., Topolnik, L., Lacaille, J. C., and McBain, C. J. (2006) *Neuron* **52,** 497–510
35. Sorensen, S. D., Macek, T. A., Cai, Z., Saugstad, J. A., and Conn, P. J. (2002) *Mol. Pharmacol.* **61,** 1303–1312
36. Okamoto, N., Hori, S., Akazawa, C., Hayashi, Y., Shigemoto, R., Mizuno, N., and Nakanishi, S. (1994) *J. Biol. Chem.* **269,** 1231–1236
37. Rebecchi, M. J., and Pentyala, S. N. (2000) *Physiol. Rev.* **80,** 1291–1335
38. Hwang, J. I., Oh, Y. S., Shin, K. J., Kim, H., Ryu, S. H., and Suh, P. G. (2005) *Biochem. J.* **389,** 181–186
39. Cockcroft, S. (2006) *Trends Biochem. Sci.* **31,** 4–7
40. Pelkey, K. A., Topolnik, L., Yuan, X. Q., Lacaille, J. C., and McBain, C. J. (2008) *Neuron* **60,** 980–987
41. Castillo, P. E., Schoch, S., Schmitz, F., Südhof, T. C., and Malenka, R. C. (2002) *Nature* **415,** 327–330
42. Lonart, G., Schoch, S., Kaeser, P. S., Larkin, C. J., Südhof, T. C., and Linden, D. J. (2003) *Cell* **115,** 49–60
43. Andrews-Zwilling, Y. S., Kawabe, H., Reim, K., Varoqueaux, F., and Brose, N. (2006) *J. Biol. Chem.* **281,** 19720–19731
44. Sansig, G., Bushell, T. J., Clarke, V. R., Rozov, A., Burnashev, N., Portet, C., Gasparini, F., Schmutz, M., Klebs, K., Shigemoto, R., Flor, P. J., Kuhn, R., Knoepfel, T., Schroeder, M., Hampson, D. R., Collett, V. J., Zhang, C., Duvoisin, R. M., Collingridge, G. L., and van der Putten, H. (2001) *J. Neurosci.* **21,** 8734–8745
45. Zhang, C. S., Bertaso, F., Eulenburg, V., Lerner-Natoli, M., Herin, G. A., Bauer, L., Bockaert, J., Fagni, L., Betz, H., and Scheschonka, A. (2008) *J. Neurosci.* **28,** 8604–8614
46. Ladera, C., del Godino, M. C., Martín, R., Luján, R., Shigemoto, M., Ciruela, F., Torres, M., and Sánchez-Prieto, J. (2007) *J. Neurochem.* **103,** 2314–2326
47. Martín, R., Ladera, C., Bartolomé-Martín, D., Torres, M., and Sánchez-Prieto, J. (2008) *Neuropharmacology* **55,** 464–473